

# Photoluminescence in $\text{Zn}_{1-x}\text{Co}_x\text{Se}$ under hydrostatic pressure

J. Bak, C.-L. Mak,\* and R. Sooryakumar

Department of Physics, The Ohio State University, Columbus, Ohio 43210

U. D. Venkateswaran

Department of Physics, Oakland University, Rochester, Michigan 48309

B. T. Jonker

Naval Research Laboratory, Washington, D.C. 20375

(Received 3 May 1996)

We report on low temperature measurements of the pressure dependence of the photoluminescence (PL) associated with  $\text{Co}^{2+}$  in ZnSe performed in a diamond anvil cell. Two sharp emission peaks at  $\sim 2.36$  eV, labeled  $L$  and  $L'$ , show a weak redshift under pressure with rapidly decreasing peak intensities. These results, together with the excitation energy and temperature dependence of the PL at 1 bar, allow for a critical examination of previous models proposed for these optical transitions. The PL data are discussed within the framework of conventional crystal-field theory based on the Racah and crystal-field parameters  $B$ ,  $C$ , and  $\Delta (=10Dq)$ . From this analysis, the normalized energy  $E/B$  is determined as a function of the normalized crystal field parameter  $Dq/B$ . Thus quantitative estimates for the enhancement in the  $p$ - $d$  hybridization with pressure (evident in the line-shape profiles of the spectra) are deduced. The energy separation between  $L$  and  $L'$  decreases continuously for modest pressures ( $\sim 1$  GPa), and raises questions about the role of spin-orbit coupling in accounting for the splitting of this emission doublet. [S0163-1829(96)07332-8]

## I. INTRODUCTION

Diluted magnetic semiconductors (DMS's) possess an interesting combination of magnetic and semiconducting properties and have thus received much recent attention.<sup>1</sup> The primary difference between transition metal dopants in DMS's and other more common shallow hydrogenic impurities in semiconductors is that the optical properties of DMS's are greatly influenced by the  $3d$  crystal levels. Furthermore, the presence of strong exchange interactions ( $s$ , $p$ - $d$ ) between the extended  $s$ - and  $p$ -band electrons and the localized  $d$  electrons as well as the intraion ( $d$ - $d$ ) interactions modify the character of these crystal-field levels. This brings about another interesting dimension to the study of DMS's. While manganese-based II-VI compounds have been most studied, high quality epitaxial films of ZnSe doped with iron<sup>2</sup> and cobalt<sup>3</sup> have also been fabricated. Compared to Mn and Fe, Co doping in ZnSe results in stronger  $s$ ,  $p$ - $d$ , and  $d$ - $d$  couplings.<sup>4</sup>

In this study we focus on ZnSe doped with cobalt (ZnSe:Co). Due to the cubic crystal field, the  $^4F$  ground term of the free  $\text{Co}^{2+}$  ion splits into a low lying singlet ( $^4A_2$ ) and two triplet ( $^4T_1$  and  $^4T_2$ ) states; spin-orbit interaction splits these levels further. Similarly, the excited states of  $\text{Co}^{2+}$  derived from  $S = \frac{1}{2}$  and  $\frac{3}{2}$  and permissible values of the orbital angular momentum are also subject to crystal-field and spin-orbit splitting. While different calculations<sup>5-7</sup> of the energy levels of  $\text{Co}^{2+}$  in ZnSe generally agree in their prediction of the relative ordering of levels, the magnitude of the crystal-field energies, particularly of the spin doublets, are model dependent.

In general, it is not known how to place the manifold of  $\text{Co}^{2+}$  (or other  $3d$  dopant) levels with respect to the host

band edges, and it is necessary to rely on experiments to make this determination. Figure 1 shows, schematically, several relevant electronic states involved in the observed optical transitions in  $\text{Zn}_{1-x}\text{Co}_x\text{Se}$ . For instance, electroabsorption<sup>8</sup> and photoluminescence<sup>9</sup> (PL) measurements place the ground-state ( $^4A_2$ ) energy level of  $\text{Co}^{2+}$  at 2.565 eV below the conduction-band edge of ZnSe. Optical absorption and luminescence connecting the singlet ground ( $^4A_2$ ) and triplet states [ $^4T_2(F)$ ,  $^4T_1(F)$ , and  $^4T_1(P)$ ] of  $\text{Co}^{2+}$  in ZnSe have been observed at  $\sim 0.409$ , 0.689, and 1.628 eV.<sup>10</sup> Three additional sharp higher-energy absorption

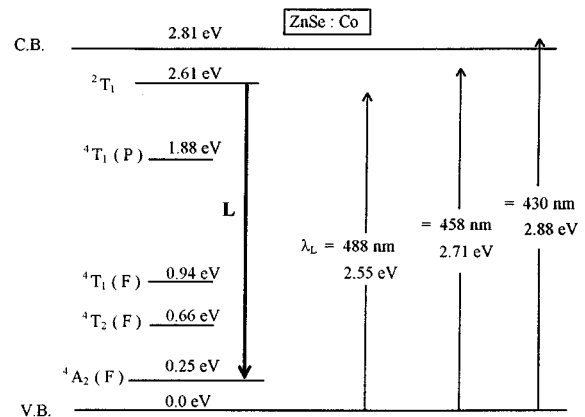


FIG. 1. Schematic energy-level diagram for  $\text{Co}^{2+} 3d^7$  multiplets in ZnSe. Only those levels involved in the observed PL transitions are shown for clarity. The location of the ground state with respect to the valence band has been determined from experiments. Also shown is the transition  $L$  and the exciting laser energies utilized in this study.

transitions labeled<sup>9</sup>  $L$ ,  $M$ , and  $N$  in the 2.35–2.55-eV region have also been reported.<sup>8,11</sup> While the absorption peak  $L$  at 2.361 eV is also evident in photoluminescence, PL transitions corresponding to  $M$  and  $N$  are not clearly observed.

Two models have emerged to account for the absorption peaks  $L$  (2.361 eV),  $M$  (2.432 eV), and  $N$  (2.546 eV). In the first, Robbins and co-workers proposed<sup>9</sup> that in absorption these zero-phonon lines initiate from the  ${}^4A_2(F)$  ground state of the  $e_g t_{2g}^3$  configuration, and terminate at unusual charge-transfer states of the  $\text{Co}^{2+}$  impurity. In this case an electron excited from a  $\text{Co}^{2+}$   $d$  orbital is localized to an orbital split off from a conduction-band minimum. The final state is characterized by two relatively weakly coupled parts: (a) the residual impurity core  $\text{Co}^{3+}$ , which gives rise to a number of different crystal-field-split electronic states, and (b) the bound-electron moving in an orbit derived largely from the host (ZnSe) conduction-band levels. Within this model  $L$ ,  $M$ , and  $N$  result from a donor-type bound state associated with these levels. This assignment was in agreement with Zeeman measurements and uniaxial stress dependence of peak  $L$ .<sup>9</sup>

In a second model,<sup>7,8,11</sup> Noras, Szawleska, and Allen<sup>11</sup> argued that  $L$ ,  $M$ , and  $N$  are at the appropriate energy where intra- $\text{Co}^{2+}$  transitions from the spin-quartet ground state  ${}^4A_2$ , to the spin-doublet-excited states (e.g.,  ${}^2T_1$ ) occur; these doublet levels lie just below or in the host conduction band. In order to account for the finite oscillator strength in these apparently spin-forbidden transitions, it was proposed that<sup>11</sup> transitions gain intensity from the presence of states with ( $d^6n$ ) configuration in the  ${}^2T_1$  state that leads to an admixture of spin- $\frac{3}{2}$  character to the spin-doublet level.

In addition to the luminescence peak  $L$  at 2.361 eV, fine structure in the form of an additional weak emission peak (labeled  $L'$ ) was observed at 2.363 eV. In the model of Ref. 9, this structure was accounted for in terms of a spin-dependent interaction between the loosely bound electron and the spin-orbit components of the remaining  $\text{Co}^{3+}$  core. O'Neill and Allen<sup>7</sup> showed that the symmetries of the spin-orbit-split level of the  ${}^2T_1$  state were consistent with the symmetries ( $E'$ ,  $U'$ ) of  $L$  and  $L'$  as reflected by Zeeman and uniaxial stress measurements.<sup>9</sup>

In this paper we focus on the hydrostatic pressure ( $P$ ) and temperature dependence of the PL transitions in  $\text{Zn}_{1-x}\text{Co}_x\text{Se}$  in the region between 2.3 and 2.4 eV, where peaks  $L$  and  $L'$  occur. Pressure is particularly useful to tune the host ZnSe band structure that allows for a critical examination of the models proposed for  $L$  and  $L'$ . If, as suggested in Ref. 9, donor-type quasihydrogenic levels are associated with  $L$ , then  $L$  should be sensitive to the movement of the host ZnSe conduction band with pressure. Moreover, pressure tunes the  $s$  and  $p$ - $d$  hybridization between the dopant and host levels by changing the relative positions of the band edges and the  $\text{Co}^{2+}$  crystal-field levels. Thus if intraion transitions<sup>11</sup> do connect spin-doublet–spin-quartet states, then the spin-quartet admixture to the  ${}^2T_1$  level will be modified by pressure; such a renormalization of the character of the admixed state should be reflected in the oscillator strength of the PL transitions. In addition, since spin-orbit couplings are not strongly modified with modest pressures, the energy separation between peaks  $L'$  and  $L$  should be

largely unaffected by a few GPa pressure if the associated levels are indeed spin-orbit components. Our experiments, that exploit pressure, temperature, and resonant laser excitation, are found to be consistent with the assignment of  $L$ ,  $M$ , and  $N$  to intra- $\text{Co}^{2+}$  transitions, as proposed<sup>11</sup> by Noras, Szawleska, and Allen. Direct evidence of changes in the  $p$ - $d$  hybridization with pressure are evident in the spectral line shapes as well as in quantitative estimates of  $dB/dP$ , the rate of change of the Racah parameter  $B$  with  $P$ . Moreover, the extreme sensitivity of the splitting between  $L$  and  $L'$  to pressure questions the role of spin-orbit coupling in exclusively accounting for these doublet emission structures.

In Sec. II we provide details of the experiment, including sample characteristics and details of the high-pressure measurements. Section III describes the experimental data and is followed by a discussion of results. The conclusions are presented in Sec. V.

## II. EXPERIMENTAL DETAILS

Epitaxial films of  $\text{Zn}_{1-x}\text{Co}_x\text{Se}$  with three different Co concentrations were grown on (001) GaAs substrates by molecular-beam epitaxy.<sup>3</sup> The layer thicknesses of the  $x=0.76\%$ , 1.6%, and 3.7% samples determined by energy-dispersive x-ray fluorescence were 2.6, 1.6, and 0.29  $\mu\text{m}$ , respectively. X-ray measurements confirmed that the films have zinc-blende structure, and were oriented with the [001] direction normal to the surface. The epilayers generally exhibit some degree of tetragonal distortion which increases with decreasing thickness or increasing concentration.<sup>12</sup> Magnetometry data confirm that the dopant Co was incorporated in a random, substitutional manner into ZnSe.<sup>13</sup>

For PL measurements at low temperature, the samples were mounted on the cold finger of a liquid-helium cryostat using a thermally conducting grease. Temperature was measured using a sensor mounted near the sample. Luminescence spectra were recorded using two spectroscopic systems; for excitation below the fundamental band gap of ZnSe, 5 mW of 514.5-, 488-, and 458-nm laser lines was utilized. A double monochromator and standard photon-counting electronics were used for detection. For excitation between 460 and 430 nm (2.70 and 2.88 eV), a dye laser (Coherent Inc., Model 702-2) using stilbene 420 dye was employed. The dye laser was pumped by a frequency-doubled, mode-locked Nd-YAG (yttrium aluminum garnet) laser operating in the continuous-wave mode. PL was excited with a power of 5 mW, and the emission was dispersed through a single-grating (600 grooves/mm) monochromator and detected by a charge-coupled device multichannel analyzer (Photometrics CC 200 with Thomson-CSF 576 x 384 pixels chip).

In order to compare the PL intensities using the two different photon detection systems, spectra of all three samples were recorded at 458 nm (2.88 eV) with both instruments. The average intensity at  $\sim 2.35$  eV for the  $x=0.76\%$  sample (at 10 K) recorded with the multichannel instrument was normalized to that obtained in the single-channel measurement at this excitation wavelength. The *same* scale factor was used for normalizing PL spectra at all other excitation wavelengths for the three samples.

For high-pressure measurements,<sup>14</sup> the samples were

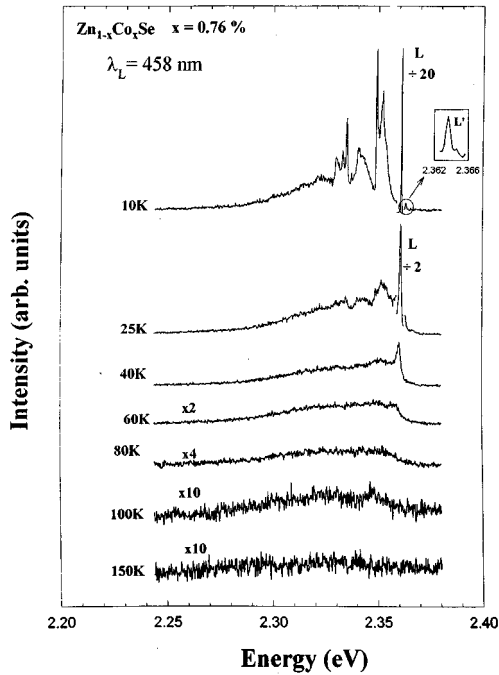


FIG. 2. Temperature dependence of the photoluminescence spectra excited with 458-nm radiation recorded for 0.76% sample. The inset shows the weak transition  $L'$  at 10 K.

thinned by mechanical lapping and polishing from the substrate side to a total thickness of  $\sim 30 \mu\text{m}$ . Square pieces typically  $\sim 75 \mu\text{m}$  on a side were chosen under an optical microscope for loading into a Merrill-Bassett-type diamond-anvil cell. The pressure chamber was formed by a  $200\text{-}\mu\text{m}$  hole drilled in a prepressed stainless-steel gasket to a thickness of  $\sim 100 \mu\text{m}$ . A thinned  $\text{Zn}_{1-x}\text{Co}_x\text{Se}$  sample and small ruby pieces were placed in the gasket hole before filling a 4:1 methanol-ethanol mixture which served as the pressure-transmitting medium. Pressure was applied at room temperature and calibrated at low temperature using a ruby  $R$ -line fluorescence shift of  $7.53 \text{ cm}^{-1}/\text{GPa}$ . Corrections due to temperature shifts were made by measuring the  $R$ -line frequencies of ruby chips inside the diamond cell, as well as from a chip attached outside the cell at each pressure. As seen from the linewidths of the ruby  $R$  lines, pressure was found to be hydrostatic to within  $\pm 0.1 \text{ GPa}$  at the highest pressure attained. Near-backscattering geometry was employed for the measurements. All data were taken in the zinc-blende phase of  $\text{ZnSe}$ , with the pressure kept below the structural transition pressure<sup>15</sup> of 13.5 GPa.

### III. EXPERIMENTAL RESULTS

Figure 2 shows the PL peaks between 2.24 and 2.38 eV for the  $x=0.76\%$  sample at 10 K, as well as their temperature dependence. The spectra were excited with the 458-nm laser line. A sharp (full width at half maximum intensity  $\sim 0.6 \text{ meV}$ ) zero-phonon line labeled  $L$  at 2.3616(3) eV is observed at 10 K. The broad structure on the low-energy side of  $L$  reflects the phonon density of states<sup>16</sup> of  $\text{ZnSe}$ , and has been previously attributed to phonon replicas.<sup>9</sup> The weaker peak  $L'$  at 2.3637(4) eV is evident at the lowest temperature.

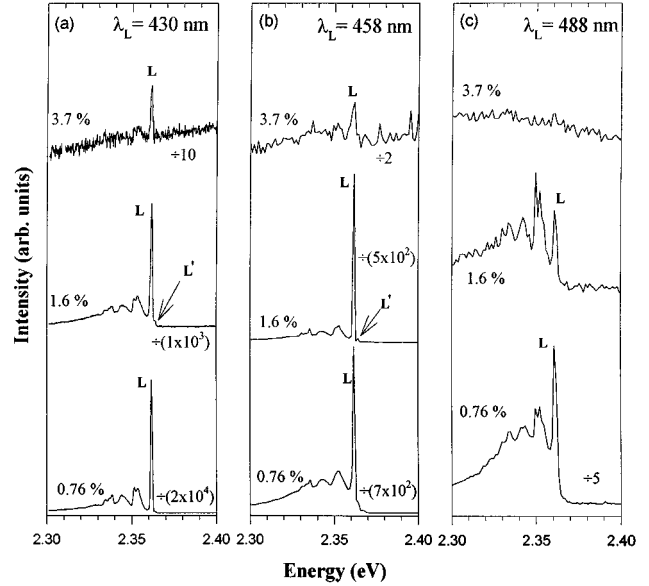


FIG. 3. Photoluminescence spectra recorded at 10 K for  $\text{Zn}_{1-x}\text{Co}_x\text{Se}$  with  $x = 0.76\%$ , 1.6%, and 3.7% excited with 5 mW of (a) 430-nm, (b) 458-nm, and (c) 488-nm laser lines. Peak  $L$  is most intense in the 0.76% sample for excitation at 430 nm. Peak  $L'$  is not observed in all spectra due to its inherent weakness and large step size taken in recording the data.

On raising the temperature,  $L$  weakens rapidly, and around 60 K it is indistinguishable from the phonon replicas that are evident until about 100 K.

The dependence of the 10-K PL on exciting laser wavelength ( $\lambda_L = 430, 458, \text{ and } 488 \text{ nm}$ ) from three  $\text{Zn}_{1-x}\text{Co}_x\text{Se}$  epilayers with  $x = 0.76\%$ , 1.6%, and 3.7% are shown in Figs. 3(a), 3(b), and 3(c). An intensity increase is observed with decreasing  $\lambda_L$  in the  $x = 3.7\%$  film, while the increase is most pronounced in the  $x = 0.76\%$  sample. For a given excitation wavelength, the PL is found to be strongest in the  $x = 0.76\%$  sample, less intense in the  $x = 1.6\%$  sample and very weak or absent in the  $x = 3.7\%$  sample.<sup>17</sup> The weak shoulder  $L'$  at 2.364 eV is not clearly evident in all spectra of Fig. 3, due to its inherent low intensity and the large step sizes ( $10 \text{ cm}^{-1}$ ) taken in recording this data.

Next we turn to the hydrostatic pressure dependence of the PL transitions  $L$  and  $L'$ . PL spectra from the  $x = 1.6\%$  sample at 10 K excited with a 458-nm laser for several pressures between 1 bar and 2.6 GPa are shown in Fig. 4. As the applied pressure ( $P$ ) increases,  $L$  and  $L'$  shift to lower energies and the intensity weakens steadily. A slightly larger redshift is apparent for  $L'$  compared to  $L$  in Fig. 4, which results in the two peaks possibly merging for pressures around 2.5 GPa. Beyond 2.6 GPa, the PL is barely observed, and is submerged in the background diamond luminescence from the anvil.

An interesting feature of peak  $L$  is its asymmetric line-shape on the low-energy side that, with increasing pressure, acquires an even greater asymmetry. A similar asymmetric line shape was observed in our earlier high-pressure studies of the LO phonons in  $\text{ZnSe}:\text{Co}$ .<sup>18</sup> Such a profile is characteristic of a Fano line shape,<sup>19</sup> and is indicative of coupling between a discrete transition and a continuum of states.

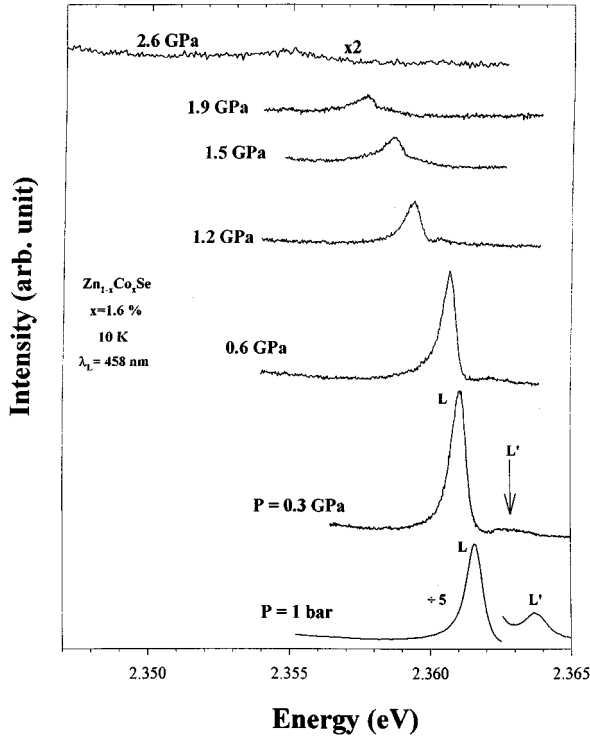


FIG. 4. Hydrostatic pressure ( $P$ ) dependence of the photoluminescence at  $\sim 2.36$  eV recorded at 10 K for the  $x = 1.6\%$  sample. Spectra were excited with 5 mW of 458-nm radiation, and are displaced for clarity.

Hence, in fitting the data of Fig. 4, we have utilized the Fano line shape given by  $I(\epsilon, q) = I_o (q + \epsilon)^2 / (1 + \epsilon^2)$ , where  $I_o$  is a constant, and  $\epsilon = (\omega - \Omega - d\Omega) / \Gamma$ . Here  $\Omega$  is the unrenormalized transition energy, and  $d\Omega$  is the shift of the transition energy due to coupling to the continuum.  $\Gamma$  is related to the full width at half maximum;  $\Gamma_{\text{FWHM}} = 2\Gamma(q^2 + 1) / (q^2 - 1)$ . The magnitude of  $q$  reflects the degree of skewness from a Lorentzian with the asymmetry increasing as  $|q|$  decreases. The peak positions of  $L$  and  $L'$  at each pressure were obtained by fitting  $L$  to a Fano and  $L'$  to a Gaussian profile. The results are summarized in Fig. 5, with filled circles denoting  $L$  and filled squares denoting  $L'$ .

The solid lines through the data of Fig. 5 are results of a least-square fit with expressions  $E_L = E_{0L} + \alpha P + \beta P^2$  and  $E_{L'} = E_{0L'} + \alpha' P + \beta' P^2$ . The coefficients  $\alpha$ ,  $\beta$ ,  $\alpha'$ , and  $\beta'$  deduced from the fits are  $-1.20$  meV/GPa,  $-0.50$  meV/GPa<sup>2</sup>,  $-2.33$  meV/GPa, and  $-0.31$  meV/GPa<sup>2</sup>, respectively. The larger error bars associated with  $L'$  for  $P \geq 1$  GPa are due to the weakness of this PL transition. The linewidth  $\Gamma_{\text{FWHM}}$ , and the Fano asymmetry parameter  $q$  of peak  $L$  deduced from the fits, are shown in the insets to Fig. 5. While  $\Gamma_{\text{FWHM}}$  of  $L$  is small ( $\sim 5$  cm<sup>-1</sup>) at low pressures, it begins to increase rapidly around 0.5 GPa, that continues to broaden to  $\sim 15$  cm<sup>-1</sup> until  $\sim 3$  GPa. The increased asymmetry of  $L$  with pressure is reflected in the steady reduction of  $|q|$  from  $\sim 7$  to 2 as  $P$  increases to 2 GPa.

#### IV. DISCUSSION

The pressure-dependent data (Fig. 5) allow one readily to discriminate between the two proposed models alluded to in

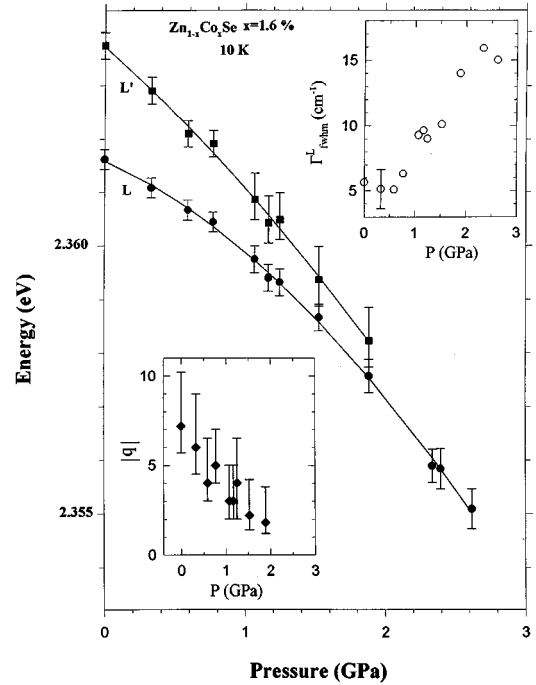


FIG. 5. The energy positions of PL transitions  $L$  and  $L'$  as a function of pressure, deduced from fits to their emission profiles. Fano and Gaussian-line shapes were utilized in describing  $L$  and  $L'$ , respectively for  $P \leq 2.0$  GPa. When  $P \geq 2.2$  GPa, the oscillator strength of  $L$  and  $L'$  are very weak; a single Gaussian profile was hence utilized to fit spectra above 2.2 GPa. The upper inset shows the width  $\Gamma_{\text{FWHM}}^L$  of peak  $L$ , while the lower inset represents the Fano asymmetry parameter  $q$  as a function of pressure.

Sec. I for the origin of  $L$ , and establish that the bound-electron model<sup>9</sup> is unlikely. Optical-absorption studies have shown that the host (ZnSe) band gap shifts<sup>15</sup> at  $+72$  meV/GPa, and hence a charge-transfer state split off from the conduction-band minimum would be expected to blueshift at a similar rate. The small *redshift* of  $\alpha = -1.20$  meV/GPa displayed by  $L$  is thus not consistent with the unusual charge-transfer state mediating the transition as proposed in Ref. 9. Another difficulty of this model is also evident in the temperature dependence shown in Fig. 2. The relatively rapid quenching of  $L$  above 100 K would imply a donor-type binding energy of  $\sim 9$  meV. On the other hand, while the  $^4A_2$  ground state has been established to lie 2.565 eV below<sup>8,9</sup> the conduction band of ZnSe, the peak position of  $L$  at 2.361 eV at ambient pressure would imply a much stronger binding; the latter is clearly not consistent with the rapid quenching of peak  $L$  evident in Fig. 2.

On the other hand, our data are consistent with the optical features arising from transitions between intraionic crystal-field levels. The redshifts observed under pressure are not unusual for intra-atomic transitions.<sup>20,21</sup> As noted earlier, it has been proposed by Noras, Szawelska, and Allen<sup>11</sup> that the  $^2T_1 \rightarrow ^4A_2$  spin-forbidden transition gains oscillator strength by the state  $^2T_1$ , acquiring a spin-quartet character arising from  $d$  levels of  $\text{Co}^{3+}$  plus the ionized electron in the conduction band. The rapid drop in intensity of peak  $L$  with pressure (Fig. 4) is consistent with this model. With increasing pressure, not only does the conduction band separate further from the local  $d$  levels, but increasingly higher exci-

tation energies are needed to remove and transfer a  $d$  electron from  $\text{Co}^{2+}$  to the conduction band. This would result in a decrease of level mixing between resonant states in the conduction band and  ${}^2T_1$ . As a result of the consequent suppression of the spin-quartet character to  ${}^2T_1$ , the oscillator strength of  $L$  decreases, as observed, with increasing pressure. In addition, upon compression, the top of the valence band moves up with respect to vacuum and hence would approach the  ${}^4A_2$  ground state. Thus hybridization between the  $3d$  Co ( ${}^4A_2$ ) and  $4p$  Se will be enhanced with pressure. A direct consequence of such  $p$ - $d$  mixing will result in a broadening of the PL emission, as evidenced by the upper inset to Fig. 5.

The connection to intra-Co transitions is further borne out in the resonant PL spectra of Fig. 3 carried out at ambient pressure. For instance, for a given Co concentration,  $L$  is strongest when excited at energies that approach or lie beyond the band gap of ZnSe. At  $\lambda_L = 430$  nm (2.88 eV),  $L$  is strongest, since  $\text{Co}^{2+}$  is ionized most effectively via  $d$ -electron transfer to the conduction band in this resonant excitation case. Similarly, the intensity of  $L$  in our experiments drops rapidly as the excitation energy decreases from 2.88 to 2.55 eV, since the ionization of  $\text{Co}^{2+}$  is suppressed and thereby the admixture of spin- $\frac{3}{2}$  character to the  ${}^2T_1$  state is reduced; the spin-forbidden  ${}^2T_1 \rightarrow {}^4A_2$  transition is hence further weakened.

In order to understand the redshifts of  $L$  and  $L'$  under pressure as well as the small magnitude of  $dE_L/dP$  ( $\alpha = -1.20$  meV/GPa and  $\beta = -0.50$  meV/GPa<sup>2</sup>), we turn to the conventional crystal-field (BC $\Delta$ ) theory developed by Sugano and Tanabe.<sup>22,23</sup> In this theory,  $B$  and  $C$  are Racah parameters that describe the Coulomb and exchange interaction between the  $3d$  electrons, and  $\Delta$  ( $=10Dq$ ) is determined by the crystal-field splitting. The ratio  $C/B$  lies between 3 and 5. By diagonalizing the Coulomb energy matrices, the crystal-field levels are determined.

We utilize the measured energy of spin-allowed, low-energy spin-quartet–spin-quartet transitions to determine  $B$  and  $\Delta$  by calculating the energies of the  ${}^4T_1$  and  ${}^4T_2$  levels with respect to the  ${}^4A_2$  ground level. The best agreements with the three measured transition energies<sup>10</sup> at 0.409, 0.689, and 1.628 eV [solid dots in Fig. 6(a)] are obtained for  $B=74.5$  meV and  $\Delta = 401.1$  meV. With these values for  $B$  and  $\Delta$ , we take the Racah parameter  $C$  as an adjustable parameter to provide a theoretical manifold of levels that best matches the specific  ${}^2T_1$  crystal-field level to the experimental value of  $E_L$  (2.361 eV at 1 bar). We assign this state to  ${}^2T_1(3)$ .<sup>24</sup> This analysis establishes the value of  $C = 368.2$  meV ( $C/B = 4.94$ ) and, in turn, allows all crystal-field levels of  $\text{Co}^{2+}$  in ZnSe to be mapped. The result is shown in Fig. 6(a).

The pressure derivative of the transition energy  $E$  between such crystal-field-split levels can be written as<sup>21</sup>

$$\frac{dE}{dP} = \delta \frac{d}{dP}(Dq) + (E - \delta Dq) \frac{1}{B} \frac{dB}{dP}. \quad (1)$$

The term  $\delta$  is given by the slope of the normalized energy  $E/B$  versus the normalized crystal-field parameter  $Dq/B$ . For  $d$ - $d$  transitions between levels that do not involve a change of electron configuration,  $E$  is independent of  $Dq$ ,

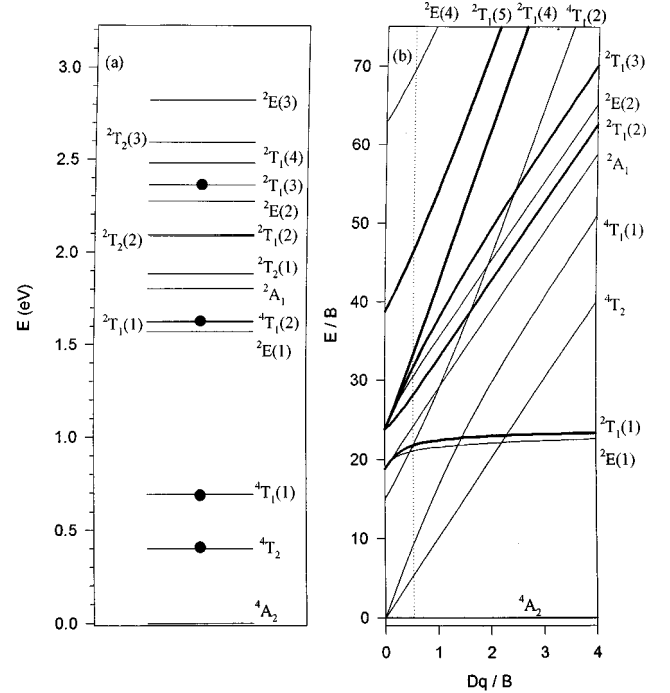


FIG. 6. (a) Calculated crystal-field energy levels of  $\text{Co}^{2+}$  in ZnSe following BC $\Delta$  theory. The solid dots indicate measured transition energies. The three spin-allowed low-lying transitions from Ref. 12 enabled  $B$  and  $\Delta$  ( $=10Dq$ ) to be determined, while the energy of  $L$  was utilized to fix  $C$  (see text). The numbers in the parentheses of specific levels indicate the order of the energy eigenvalue from the lowest level of the same symmetry. (b) Sugano-Tanabe diagram deduced from the crystal-field levels of (a), providing the normalized energy  $E/B$  as a function of the normalized crystal field parameter  $Dq/B$ . The thicker lines identify all five  ${}^2T_1$  levels. Some levels are omitted for clarity. These include all  ${}^2T_2$  states and the  ${}^2E(3)$  state.

and thus  $\delta$  is zero. In this special case the first term of Eq. (1) vanishes. As shown below, this is not the situation for transition  $L$  in ZnSe:Co.

For values of  $B$  and  $C$ , we calculate the normalized energy  $E/B$  as a function of  $Dq/B$ . Figure 6(b) shows the resulting Sugano-Tanabe diagram corresponding to the energy levels depicted in Fig. 6(a). The thicker lines in Fig. 6(b) are associated with the  ${}^2T_1$  levels. The energy of the lowest level  ${}^2T_1(1)$  has minimal variation with  $Dq$ , since its electronic configuration is similar to that of the ground state  ${}^4A_2$ . The dotted line represents the value  $Dq/B=0.538$ , a ratio that, as noted above, is determined from the low-lying spin-allowed transitions. The slope of the curve labeled  ${}^2T_1(3)$  at  $Dq/B=0.538$  is the value of  $\delta$  associated with  $E_L$ . We find  $\delta = +13.3$ .

Since the crystal-field splitting  $Dq$  is proportional to  $a^{-5}$ , where  $a$  is the lattice parameter,<sup>25</sup> the pressure derivative of  $Dq$  for cubic crystals can be written as<sup>21</sup>  $d(Dq)/dP = 5Dq\kappa/3$ , with the compressibility  $\kappa$  of the ZnSe film taken<sup>26</sup> as  $1.53 \times 10^{-2}$  GPa<sup>-1</sup>. Thus the value of  $\delta d(Dq)/dP$  in Eq. (1) is  $+13.6$  meV/GPa.

With the knowledge of  $dE/dP = -2.7$  meV/GPa at  $P = 1.5$  GPa from Fig. 5, and values of  $Dq$ ,  $\delta$ , and  $B$  determined above, it follows from Eq. (1) that  $dB/dP = -0.66(5)$  meV/

GPa. This negative pressure coefficient of the Racah parameter directly reflects an enhancement of the hybridization between the  $\text{Co}^{2+}$  and the host states with increasing pressure. In ZnSe:Co, such an increase in hybridization is a direct manifestation of the close proximity of the  ${}^4A_2$  ground state to the valence-band maximum. With increasing pressure, the valence-band maximum moves up and couples with the lowest crystal-field level. A preliminary report of the pressure induced enhancement in the  $p$ - $d$  hybridization in ZnSe:Co was presented earlier.<sup>27</sup>

We now discuss the weaker peak  $L'$  (Figs. 4 and 5) that lies 2 meV above  $L$  at 1 bar. For relatively low pressures ( $P < 1.5$  GPa) it is clear that the energy separation between  $L$  and  $L'$  decreases as  $P$  rises. At higher pressures, due to the weakened intensities, their peak positions are determined to a lesser degree of confidence as reflected by the larger error bars in Fig. 5. Hence, while it is difficult to unambiguously conclude if  $L$  and  $L'$  do become degenerate around 2.5 GPa, it is clear that the splitting between these modes is sensitive to pressure, and is reduced continuously between 1 bar and 2 GPa.

Peak  $L'$  has been previously attributed<sup>7</sup> to the spin-orbit split component of  $L$ . In order to account for the pressure data of Fig. 5, however, such an assignment to  $L'$  would require that the orbital angular momentum of the  $d$  electrons be sensitive to and suppressed by modest hydrostatic pressures that, in turn, lead to reductions in the spin-orbit splitting. This is unlikely, and thus the proposal<sup>7</sup> that spin-orbit coupling is the sole origin for the 2-meV splitting between  $L$  and  $L'$  at ambient pressure is doubtful. *Additional* effects, such as the differing hybridization of the two spin-orbit components, could contribute to the separation. For instance, the level in the conduction band providing the spin-quartet admixture associated with transition  $L$  should couple differently to the second spin-orbit component because of its different symmetry and energy. With increasing hydrostatic pressure, such a hybridization of the two components would be suppressed to different extents, and could result in the separation between  $L$  and  $L'$  being sensitive to pressure.

As another possibility for the origin of  $L'$ , we suggest the presence of metastable off-center sites for  $\text{Co}^{2+}$  in ZnSe. Off-center sites<sup>28</sup> resulting from Jahn-Teller-type instabilities have been found in I-VII zinc-blende semiconductors such as CuCl and CuBr. The vibronic character noted<sup>9</sup> for  $L'$  as well as some tetragonal distortion observed in x-ray data from our films<sup>12</sup> support the view that Jahn-Teller interactions and hence off-center sites for Co in ZnSe are possible. Electron paramagnetic resonance data<sup>13</sup> from the 0.76% sample, for

example, show a strong angular dependence which has been attributed to the occupation of reduced symmetry sites. The crystal fields experienced by  $\text{Co}^{2+}$  ions located at these two (on- and off-center) sites will be different, leading to two transitions ( $L$  and  $L'$ ). The large intensity difference between  $L$  and  $L'$  at ambient pressure would be a reflection of the ratio of Co ions at each of these two types of sites, as well as the character of the associated level wave functions. The merging of these peaks with pressure (Fig. 5) would arise from reductions in the energy difference between on- and off-center sites, with the corresponding  $\text{Co}^{2+}$  ions then experiencing similar crystal fields.

## V. CONCLUSIONS

In summary, we have investigated the origin of PL transitions at  $\sim 2.36$  eV in the diluted magnetic semiconductor ZnSe:Co. The hydrostatic pressure dependence of the peak position and intensity of transition  $L$  in  $\text{Zn}_{1-x}\text{Co}_x\text{Se}$  are consistent with the emission being associated with the spin-forbidden  ${}^2T_1 \rightarrow {}^4A_2$  intra- $\text{Co}^{2+}$  transition. The rapid drop in PL intensity with pressure and the dependence on exciting laser energy are in agreement with this transition acquiring oscillator strength via admixing with states derived from  $\text{Co}^{3+}$  levels, and an electron in the conduction band. Evidence of pressure-induced enhancement of the  $p$ - $d$  hybridization is revealed in the rapid broadening of  $L$  beyond  $\sim 0.5$  GPa, when the valence band approaches and couples to the ground  ${}^4A_2$  state. This hybridization is also reflected in the value of  $dB/dP = -0.66(5)$  meV/GPa. The small redshift of  $L$  with pressure is a result of compensating contributions from the pressure dependence of crystal-field and multiplet splitting terms deduced from the Sugano-Tanabe diagram. The weak peak  $L'$ , previously assigned to the spin-orbit component of  $L$ , has a similar though slightly stronger dependence of energy on pressure. This behavior raises questions about the role of spin-orbit coupling in solely accounting for the splitting between this emission doublet.

## ACKNOWLEDGMENTS

We thank James Leonard for help in the PL measurements that utilized the charge-coupled multichannel detector system. Research at the Ohio State University was supported by the National Science Foundation under Contract No. DMR 90-01647. U.D.V. acknowledges support from Cottrell College Science Award No. CC-3293 by the Research Corporation. The work at NRL was supported by the Office of Naval Research.

\*Present address: Department of Applied Physics and Materials Research Center, The Hong Kong Polytechnic University, Hung Hom, Hong Kong.

<sup>1</sup>*Diluted Magnetic Semiconductors*, edited by J.K. Furdyna and J. Kossut, Semiconductors and Semimetals Vol. 25, edited by R.K. Willardson and A.C. Beer (Academic, San Diego, 1988); J.K. Furdyna, *J. Appl. Phys.* **64**, R29 (1988).

<sup>2</sup>B.T. Jonker, J.J. Krebs, S.B. Qadri, and G.A. Prinz, *Appl. Phys. Lett.* **50**, 848 (1987).

<sup>3</sup>B.T. Jonker, J.J. Krebs, and G.A. Prinz, *Appl. Phys. Lett.* **53**, 450 (1988).

<sup>4</sup>X. Liu, A. Petrou, B.T. Jonker, G.A. Prinz, J.J. Krebs, and J. Warnock, *Appl. Phys. Lett.* **53**, 476 (1988); X. Liu, A. Petrou, B.T. Jonker, G.A. Prinz, J.J. Krebs, and J. Warnock, *ibid.* **55**, 1023 (1989).

<sup>5</sup>A. Fazio, M.J. Caldas, and A. Zunger, *Phys. Rev. B* **30**, 3430 (1984); L.A. Hemstreet and J.P. Dimmock, *ibid.* **20**, 1527 (1979).

<sup>6</sup>M. Villeret, S. Rodriguez, and E. Kartheuser, *Physica B* **162**, 89 (1990).

<sup>7</sup>A.G. O'Neill and J.W. Allen, *Solid State Commun.* **46**, 833 (1983).

- <sup>8</sup>V.I. Sokolov, T.P. Surkova, M.P. Kulakov, and A.V. Fadeev, *Phys. Status Solidi B* **130**, 267 (1985); V.I. Sokolov, A.N. Mamedov, T.P. Surkova, M.V. Chukichev, and M.P. Kulakov, *Opt. Spectrosc.* **62**, 480 (1987).
- <sup>9</sup>D.J. Robbins, P.J. Dean, C.L. West, and W. Hayes, *Philos. Trans. R. Soc. London Ser. A* **304**, 499 (1982); D.J. Robbins, P.J. Dean, J.L. Glasper, and S.G. Bishop, *Solid State Commun.* **36**, 61 (1980).
- <sup>10</sup>J.M. Baranowski, J.W. Allen, and G.L. Pearson, *Phys. Rev.* **160**, 627 (1967); E.M. Wray and J.W. Allen, *J. Phys. C* **4**, 512 (1971); S.M. Uba and J.M. Baranowski, *Phys. Rev. B* **17**, 69 (1978); A.P. Radlinski, *J. Phys. C* **13**, 2407 (1980); G. Goetz and H.-J. Schultz, *Phys. Status Solidi B* **169**, 217 (1992).
- <sup>11</sup>J.M. Noras, H.R. Szawelska, and J.W. Allen, *J. Phys. C* **14**, 3255 (1981).
- <sup>12</sup>B.T. Jonker, S.B. Qadri, J.J. Krebs, G.A. Prinz, and Salamanca-Young, *J. Vac. Sci. Technol. A* **7**, 1360 (1989); B.T. Jonker, J.J. Krebs, G.A. Prinz, X. Liu, A. Petrou, and Salamanca-Young, in *Growth, Characterization and Properties of Ultrathin Magnetic Films and Multilayers*, edited by B.T. Jonker, E.E. Marinero, and J.P. Heremans, MRS Symposia Proceedings No. 151 (Materials Research Society, Pittsburgh, 1989), p. 151.
- <sup>13</sup>J.J. Krebs, B.T. Jonker, and G.A. Prinz, *IEEE Trans. Magn.* **24**, 2548 (1988).
- <sup>14</sup>A. Jayaraman, *Rev. Mod. Phys.* **55**, 65 (1983).
- <sup>15</sup>S. Ves, K. Strössner, N.E. Christensen, C.K. Kim, and M. Cardona, *Solid State Commun.* **56**, 479 (1985).
- <sup>16</sup>K. Kunc, M. Balkanski, and M.A. Nusimovici, *Phys. Status Solidi B* **72**, 229 (1975).
- <sup>17</sup>C.-L. Mak, R. Sooryakumar, M.M. Steiner, and B.T. Jonker, *Phys. Rev. B* **48**, 11 743 (1993); C.-L. Mak, J. Bak, R. Sooryakumar, M.M. Steiner, and B.T. Jonker, *J. Appl. Phys.* **75**, 5719 (1994).
- <sup>18</sup>J. Bak, U. Venkateswaran, C.L. Mak, R. Sooryakumar, and B.T. Jonker, *J. Phys. Chem. Solids* **56**, 563 (1995).
- <sup>19</sup>U. Fano, *Phys. Rev.* **124**, 1866 (1961); M. Chandrasekhar, J.B. Renucci, and M. Cardona, *Phys. Rev. B* **17**, 1623 (1973).
- <sup>20</sup>K. Hochberger, H.H. Otto, and W. Gebhardt, *Solid State Commun.* **62**, 11 (1987); S. Ves, K. Strössner, W. Gebhardt, and M. Cardona, *ibid.* **57**, 335 (1986); D. Wasik, Z. Liro, and M. Baj, *J. Cryst. Growth* **101**, 466 (1990).
- <sup>21</sup>S. Ves, K. Strössner, W. Gebhardt, and M. Cardona, *Phys. Rev. B* **33**, 4077 (1986).
- <sup>22</sup>S. Sugano, Y. Tanabe, and N. Kamimura, in *Multiplets of Transition Metal Ions in Crystal*, edited by H.S.W. Massey and K.A. Brueckner, Pure and Applied Physics Vol. 33 (Academic, New York, 1970).
- <sup>23</sup>J.S. Griffith, *The Theory of Transition Metal Ions* (Cambridge University Press, Cambridge, 1961).
- <sup>24</sup>Note that for a different value of  $C$  ( $= 328.6$  meV), the calculated energy difference associated with the  ${}^2T_1(4) \rightarrow {}^4A_2$  transition would also provide a good match to  $L$ . In this case the  ${}^2T_1(3)$  state lies 0.118 meV below  ${}^2T_1(4)$ . This situation is unlikely, however, since the presence of  ${}^2T_1(3)$  provides another decay channel and hence a transition corresponding to  ${}^2T_1(3) \rightarrow {}^4A_2$  should be observed; such is not the case.
- <sup>25</sup>D.S. McClure, in *Solid State Physics*, edited by F. Seitz and D. Turnbull (Academic, New York, 1958), Vol. 9, p. 339.
- <sup>26</sup>B. Hillebrands, S. Lee, G.I. Stegeman, H. Cheng, J.E. Potts, and F. Nizzoli, *Phys. Rev. Lett.* **60**, 832 (1988).
- <sup>27</sup>U. Venkateswaran, C.-L. Mak, J. Bak, R. Sooryakumar, and B.T. Jonker, in *High Pressure Science and Technology – 1993*, edited by S.C. Schmidt *et al.* (American Institute of Physics, New York, 1994) pp. 593–596.
- <sup>28</sup>S.-H. Wei, S.B. Zhang, and A. Zunger, *Phys. Rev. Lett.* **70**, 1639 (1993).